arXiv:1601.00927v2 [hep-ph] 12 May 2016

Degeneracies in long-baseline neutrino experiments from nonstandard interactions

Jiajun Liao,[1] Danny Marfatia,[1] and Kerry Whisnant[2]

[1] *Department of Physics and Astronomy, University of Hawaii at Manoa, Honolulu, HI 96822, USA*
[2] *Department of Physics and Astronomy, Iowa State University, Ames, IA 50011, USA*

We study parameter degeneracies that can occur in long-baseline neutrino appearance experiments due to nonstandard interactions (NSI) in neutrino propagation. For a single off-diagonal NSI parameter, and neutrino and antineutrino measurements at a single L/E, there exists a continuous four-fold degeneracy (related to the mass hierarchy and θ_{23} octant) that renders the mass hierarchy, octant, and CP phase unknowable. Even with a combination of NOνA and T2K data, which in principle can resolve the degeneracy, both NSI and the CP phase remain unconstrained because of experimental uncertainties. A wide-band beam experiment like DUNE will resolve this degeneracy if the nonzero off-diagonal NSI parameter is $\epsilon_{e\mu}$. If $\epsilon_{e\tau}$ is nonzero, or the diagonal NSI parameter ϵ_{ee} is $\mathcal{O}(1)$, a wrong determination of the mass hierarchy and of CP violation can occur at DUNE. The octant degeneracy can be further complicated by $\epsilon_{e\tau}$, but is not affected by ϵ_{ee}.

After decades of neutrino oscillation experiments, the standard model (SM) with massive neutrinos is well established and the study of neutrino oscillations has entered the precision era [1]. Next generation neutrino oscillation experiments will be sensitive to physics beyond the SM, which is often described in a model-independent manner by nonstandard interactions (NSI); for a recent review see Ref. [2]. In general, NSI not only affect neutrino propagation in matter via neutral-current interactions, but also affect neutrino production and detection via charged-current interactions. Model-independent bounds on the production and detection NSI are generally an order of magnitude stronger than the matter NSI [3]. Therefore, we neglect production and detection NSI in this work, and focus on matter NSI, which can be described by dimension-six four-fermion operators of the form [4]

$$\mathcal{L}_{\rm NSI} = 2\sqrt{2}G_F\epsilon^{\mathfrak{f}C}_{\alpha\beta}[\overline{\nu}_\alpha\gamma^\rho P_L\nu_\beta][\overline{\mathfrak{f}}\gamma_\rho P_C\mathfrak{f}] + \text{h.c.}\,, \qquad (1)$$

where $\alpha,\beta = e,\mu,\tau$, $C = L,R$, $\mathfrak{f} = u,d,e$, and $\epsilon^{\mathfrak{f}C}_{\alpha\beta}$ are dimensionless parameters that quantify the strength of the new interaction relative to the SM. Since neutral-current interactions affect neutrino propagation coherently, the matter NSI potentially have a large effect on the long-baseline neutrino oscillation experiments, T2K [5], NOνA [6], and DUNE [7]. Previous studies of matter NSI in these experiments can be found in Refs. [8, 9].

In this paper, we use bi-probability plots and numerical simulations to analyze parameter degeneracies in long-baseline neutrino appearance experiments that arise from matter NSI. We specifically study how well the NOνA, T2K and DUNE experiments will resolve these degeneracies for the cases of one and two off-diagonal NSI, and diagonal NSI.

Oscillation probabilities. The Hamiltonian for neutrino propagation in the flavor basis may be written as

$$H = \frac{1}{2E}\left[U\,\text{diag}(0,\delta m^2_{21},\delta m^2_{31})U^\dagger + V\right]\,, \qquad (2)$$

where U is the PMNS mixing matrix [1], $\delta m^2_{ij} = m^2_i - m^2_j$, and V represents the potential arising from interactions of neutrinos in matter,

$$V = A\begin{pmatrix} 1+\epsilon_{ee} & \epsilon_{e\mu}e^{i\phi_{e\mu}} & \epsilon_{e\tau}e^{i\phi_{e\tau}} \\ \epsilon_{e\mu}e^{-i\phi_{e\mu}} & \epsilon_{\mu\mu} & \epsilon_{\mu\tau}e^{i\phi_{\mu\tau}} \\ \epsilon_{e\tau}e^{-i\phi_{e\tau}} & \epsilon_{\mu\tau}e^{-i\phi_{\mu\tau}} & \epsilon_{\tau\tau}\end{pmatrix}. \qquad (3)$$

Here, $A \equiv 2\sqrt{2}G_F N_e E$ and $\epsilon_{\alpha\beta}e^{i\phi_{\alpha\beta}} \equiv \sum_{\mathfrak{f},C}\epsilon^{\mathfrak{f}C}_{\alpha\beta}\frac{N_\mathfrak{f}}{N_e}$, with $N_\mathfrak{f}$ the number density of fermion $\mathfrak{f}$. The $\epsilon_{\alpha\beta}$ are real, and $\phi_{\alpha\beta} = 0$ for $\alpha = \beta$. The unit contribution to the ee element of the matrix is due to the standard charged-current interaction.

Expanding the $\nu_\mu \to \nu_e$ oscillation probability for the normal hierarchy (NH) in the small quantities s_{13}, r, and the nondiagonal ϵ, we find (with $c_{jk} \equiv \cos\theta_{jk}$, $s_{jk} \equiv \sin\theta_{jk}$)

$$\begin{aligned}
P(\nu_\mu \to \nu_e) &= x^2f^2 + 2xyfg\cos(\Delta+\delta) + y^2g^2 \\
&+ 4\hat{A}\epsilon_{e\mu}\left\{xf[s^2_{23}f\cos(\phi_{e\mu}+\delta) + c^2_{23}g\cos(\Delta+\delta+\phi_{e\mu})]\right. \\
&\qquad \left. + yg[c^2_{23}g\cos\phi_{e\mu} + s^2_{23}f\cos(\Delta-\phi_{e\mu})]\right\} \\
&+ 4\hat{A}\epsilon_{e\tau}s_{23}c_{23}\left\{xf[f\cos(\phi_{e\tau}+\delta) - g\cos(\Delta+\delta+\phi_{e\tau})]\right. \\
&\qquad \left. - yg[g\cos\phi_{e\tau} - f\cos(\Delta-\phi_{e\tau})]\right\} \\
&+ 4\hat{A}^2g^2c^2_{23}|c_{23}\epsilon_{e\mu} - s_{23}\epsilon_{e\tau}|^2 + 4\hat{A}^2f^2s^2_{23}|s_{23}\epsilon_{e\mu} + c_{23}\epsilon_{e\tau}|^2 \\
&+ 8\hat{A}^2fgs_{23}c_{23}\left\{c_{23}\cos\Delta\left[s_{23}(\epsilon^2_{e\mu} - \epsilon^2_{e\tau})\right.\right. \\
&\qquad \left. + 2c_{23}\epsilon_{e\mu}\epsilon_{e\tau}\cos(\phi_{e\mu}-\phi_{e\tau})\right] \\
&\qquad \left. - \epsilon_{e\mu}\epsilon_{e\tau}\cos(\Delta - \phi_{e\mu} + \phi_{e\tau})\right\} \\
&+ \mathcal{O}(s^2_{13}\epsilon, s_{13}\epsilon^2, \epsilon^3)\,, \qquad (4)
\end{aligned}$$

where following Ref. [10],

$$\begin{aligned}
&x \equiv 2s_{13}s_{23}\,, \quad y \equiv 2rs_{12}c_{12}c_{23}\,, \quad r = |\delta m^2_{21}/\delta m^2_{31}|\,, \\
&f,\,\bar{f} \equiv \frac{\sin[\Delta(1 \mp \hat{A}(1+\epsilon_{ee}))]}{(1\mp\hat{A}(1+\epsilon_{ee}))}\,,\; g \equiv \frac{\sin(\hat{A}(1+\epsilon_{ee})\Delta)}{\hat{A}(1+\epsilon_{ee})}\,, \\
&\Delta \equiv \left|\frac{\delta m^2_{31}L}{4E}\right|\,,\; \hat{A} \equiv \left|\frac{A}{\delta m^2_{31}}\right|\,. \qquad (5)
\end{aligned}$$

Note that our definitions of f, $\bar{f}$, and g here include ϵ_{ee}, which is not treated as a small parameter. We have set $c_{13} \to 1$, which is accurate up to first order in θ_{13}. The

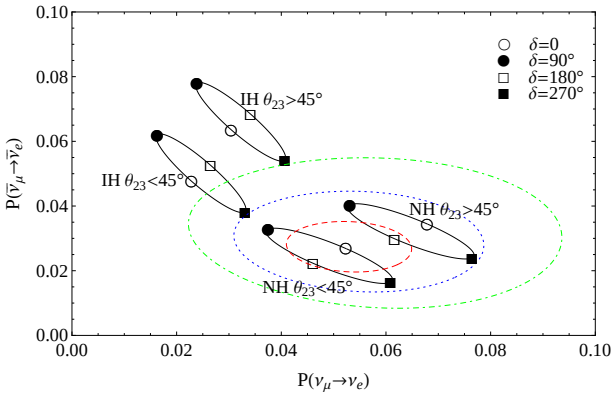

FIG. 1. Bi-probability plots ($P(\overline{\nu}_\mu \to \overline{\nu}_e)$ versus $P(\nu_\mu \to \nu_e)$) for $L = 1300$ km and $E = 3$ GeV. The solid curves show the SM values for fixed mixing angles and varying δ (one curve for each combination of hierarchy and θ_{23} octant); the dashed (dotted) [dotdashed] curves show the values assuming NSI with $\epsilon_{e\mu} = 0.05$ (0.10) [0.15], and varying $\phi_{e\mu}$ for the NH and first octant with $\delta' = 0$. The mixing angles and mass-squared differences are set at their best-fit values from Ref. [12].

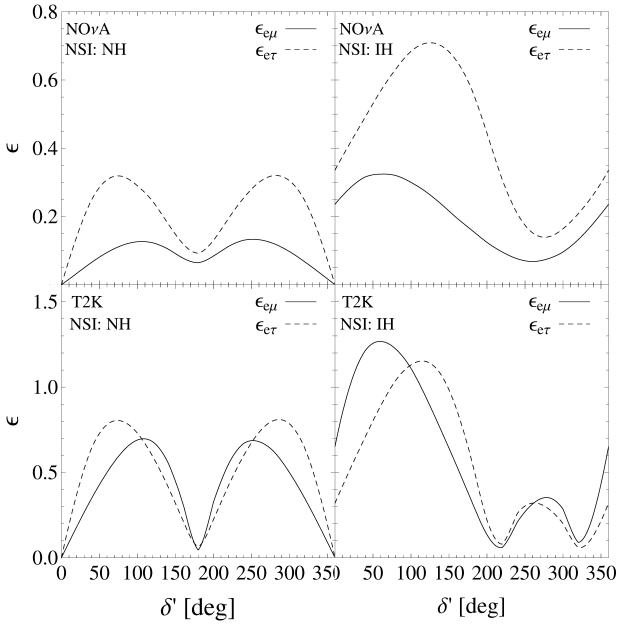

FIG. 2. Values of a single nonzero ϵ as a function of δ' that give $P(\nu_\mu \to \nu_e)$ and $P(\overline{\nu}_\mu \to \overline{\nu}_e)$ degenerate with the SM with $\delta = 0$ and NH, at NOνA ($L = 810$ km, $E = 2$ GeV) and T2K ($L = 295$ km, $E = 0.6$ GeV). The mixing angles and mass-squared differences are the best-fit values in Ref. [12].

antineutrino probability $\overline{P} \equiv P(\overline{\nu}_e \to \overline{\nu}_\mu)$, is given by Eq. (4) with $\hat{A} \to -\hat{A}$ (and hence $f \to \bar{f}$), $\delta \to -\delta$, and $\phi_{\alpha\beta} \to -\phi_{\alpha\beta}$. For the inverted hierarchy (IH), $\Delta \to -\Delta$, $y \to -y$, $\hat{A} \to -\hat{A}$ (i.e., $f \leftrightarrow -\bar{f}$, and $g \to -g$). Since s_{13} and r are small, so are x (≈ 0.2) and y (≈ 0.02). Furthermore, $\hat{A} \lesssim 0.3$ for $L \leq 1300$ km. Our result agrees with the $\mathcal{O}(\epsilon)$ expression of Ref. [11]. The 90% C.L. limits on the NSI parameters that appear in Eq. (4) are $\epsilon_{ee} < 4.2$, $\epsilon_{e\mu} < 0.33$, and $\epsilon_{e\tau} < 3.0$ [3]. The other $\epsilon_{\alpha\beta}$ do not appear in Eq. (4) up to second order in ϵ. Since Eq. (4) is only valid for small nondiagonal ϵ, in our simulations the oscillation probabilities are evaluated numerically without approximation.

One off-diagonal NSI. If $\epsilon_{ee} = 0$, and only one off-diagonal NSI in Eq. (4) (i.e., $\epsilon_{e\mu}$ or $\epsilon_{e\tau}$) is nonzero, and a measurement of the neutrino and antineutrino oscillation probability is made at one particular L and E (which is approximately true for a narrow-band beam experiment), then a parameter degeneracy between the SM and a model with NSI will occur when $P^{SM}(\delta) = P^{NSI}(\delta', \epsilon, \phi)$ and $\overline{P}^{SM}(\delta) = \overline{P}^{NSI}(\delta', \epsilon, \phi)$, where δ' is the Dirac CP phase in the model with NSI. Assuming the three mixing angles and two mass-squared differences are well-measured by other experiments, for each value of δ in the SM there are three unknowns to be determined that give an off-diagonal NSI degeneracy: δ', the magnitude ϵ and the phase ϕ. With only two constraining equations, in general there will be a continuum of solutions that can give a parameter degeneracy; i.e., for each value of δ, a solution for ϵ and ϕ will exist for *any* value of δ'.

Therefore, in the context of one off-diagonal NSI, any CP phase value is allowed with a single measurement of P and $\overline{P}$. This may be demonstrated via a bi-probability plot, which shows $\overline{P}$ versus P (see Fig. 1). The solid ellipses in Fig. 1 represent possible $\overline{P}$ and P values for the SM with fixed mixing angles and varying δ. The four ellipses are for NH and first θ_{23} octant, NH and second octant, IH and first octant, and, IH and second octant, corresponding to the usual four-fold degeneracy that remains now that the oscillation amplitudes and mass-squared differences have been measured.

The non-solid contours in Fig. 1 represent the probabilities for the same mixing angles for the NH and first octant including NSI with $\delta' = 0$, fixed ϵ and varying ϕ. The center of the non-solid contours is located at the $\delta = 0$ point of the NH-first octant solid ellipse. Clearly any point on any of the solid ellipses (i.e., any δ, either hierarchy, and either octant) can be obtained by centering the non-solid contours on any other point of the NH-first octant solid ellipse (i.e., any δ') with an appropriate value of ϵ and ϕ. In the limit where the ϵ^2 terms can be ignored, the non-solid contours are simple ellipses, the sizes of which are determined by the magnitude ϵ; when ϵ is larger, the ellipses become distorted, their range increasing with ϵ. NSI with the IH and/or second octant can be obtained similarly by centering the non-solid contours on the points of the corresponding solid ellipse.

Figure 2 shows the values of ϵ versus δ' that have a degeneracy with the SM with $\delta = 0$ and NH, for either $\epsilon_{e\mu}$ or $\epsilon_{e\tau}$, for the baseline and approximate position of the spectrum peak in the NOνA and T2K experiments, assuming NSI solutions with a NH or IH. For NOνA, these values are within the corresponding experimental

constraints for all δ'. The values of ϵ that give a degeneracy are larger in T2K since the relative size of the matter effect is smaller there due to the lower average density and shorter distance. Similar curves exist for other values of δ for the NH; in all cases, $\epsilon = 0$ when $\delta' = \delta$, but $\epsilon > 0$ when $\delta' \neq \delta$, i.e., degenerate NSI solutions only exist when $\delta' \neq \delta$. For the IH, the values of ϵ that give a degeneracy at $\delta' = 270°$ are smaller than those at $\delta' = 90°$. This can be understood from the bi-probability plot in Fig. 1: the IH with $\delta = 270°$ is closest to the NH.

Approximate formulas for the curves in the left panels of Fig. 2 can be obtained by dropping the $r\epsilon$ and ϵ^2 terms in Eq. (4):

$$\tan(\phi_{e\mu} + \delta') = \frac{s^2_{23}(f - \bar{f})}{2c^2_{23} g \sin\Delta} + \frac{\cos\Delta(\cos\delta - \cos\delta')[2c^2_{23} g \cos\Delta + s^2_{23}(f + \bar{f})]}{2c^2_{23} g \sin^2\Delta(\sin\delta - \sin\delta')}, \quad (6)$$

$$\epsilon_{e\mu} = \frac{yg[\cos(\Delta + \delta) - \cos(\Delta + \delta')]}{2\hat{A}[c^2_{23} g \cos(\Delta + \phi_{e\mu} + \delta') + s^2_{23} f \cos(\phi_{e\mu} + \delta')]},$$

and

$$\tan(\phi_{e\tau} + \delta') = \frac{(\bar{f} - f)}{2g \sin\Delta} + \frac{\cos\Delta(\cos\delta - \cos\delta')[2g\cos\Delta - f - \bar{f}]}{2g\sin^2\Delta(\sin\delta - \sin\delta')}, \quad (7)$$

$$\epsilon_{e\tau} = \frac{-yg[\cos(\Delta + \delta) - \cos(\Delta + \delta')]}{2\hat{A}s_{23}c_{23}[g\cos(\Delta + \phi_{e\tau} + \delta') - f\cos(\phi_{e\tau} + \delta')]}.$$

$\epsilon_{e\mu}$ and $\epsilon_{e\tau}$ are obtained by first solving Eqs. (6) and (7) for $\phi_{e\mu}$ and $\phi_{e\tau}$. Similar equations exist for each of the other possibilities, i.e., NSI with any δ', either hierarchy and either octant can mimic the SM with any δ, either hierarchy and either octant.

To remove the NSI degeneracies, additional measurements must be made. Since there are degeneracies throughout the two-dimensional $\delta - \delta'$ space, one additional measurement (such as a neutrino probability at a different L and/or E) will reduce the dimensionality of the degeneracies by one, i.e., to lines in $\delta - \delta'$ space. Thus for each value of δ there will only be one δ' that will be degenerate (or perhaps a finite number of δ' if there are multiple solutions). Two additional measurements at a different L and/or E will remove the degeneracies; the only solutions then are $\delta' = \delta$ and $\epsilon = 0$.

Simulations. In practice, even narrow-band beams have a spread of energies, although the energy resolution and uncertainties may not allow the degeneracies to be resolved. We simulate the long-baseline experiments using the GLoBES software [13], supplemented with the new physics tools developed in Refs. [11, 14]. We use the experimental setup for NOνA and T2K as in Ref. [15], in which T2K collects data for 5 years each in the neutrino and antineutrino mode, while NOνA runs for 3 years in each mode. For DUNE, we consider a 34 kiloton liquid argon detector with a 1.2 MW beam, and running for 3 years in each mode. We checked that our measurement

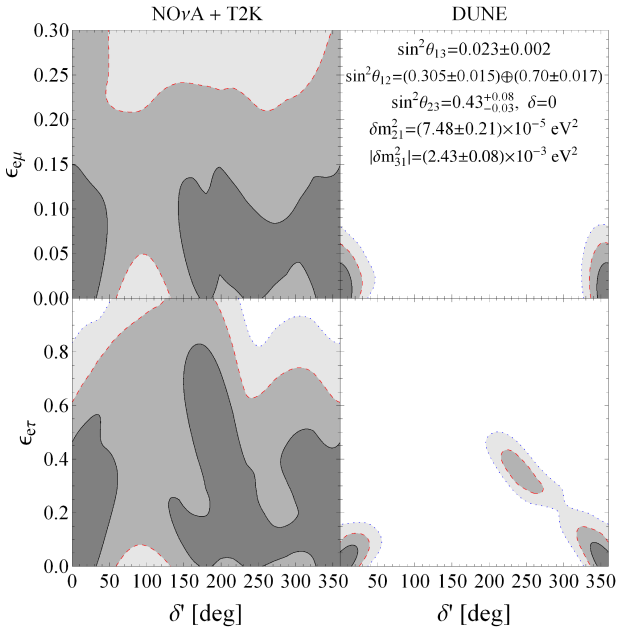

FIG. 3. 1σ, 2σ and 3σ allowed regions for $\epsilon_{e\mu}$ and $\epsilon_{e\tau}$ (when only one of them is nonzero) from combined NOνA and T2K data, and from DUNE.

precision is comparable to the projected results in Ref. [7], and the expected sensitivity for the mixing angles and mass-squared differences in our simulation match Fig. 8 of Ref. [16]. The Preliminary Reference Earth Model density profile [17] is implemented in GLoBES, and we use a conservative 5% uncertainty for the matter density [18]. Also, to be conservative, we adopt the central values and priors on the mixing angles and mass-squared differences, and the sizes of the NSI parameters in our simulation from the global-fit with NSI in Ref. [12].

In Fig. 3 we show the expected allowed regions (defined by $\Delta\chi^2$ for two degrees of freedom assuming the parameters are Gaussian distributed) in the $\delta' - \epsilon_{e\mu}$ space and $\delta' - \epsilon_{e\tau}$ space from the neutrino and antineutrino appearance channels from NOνA and T2K combined, and from DUNE. We assume that the data are consistent with the SM with $\delta = 0$, the first octant, and the NH. We scan over all octant and hierarchy combinations. Even with the NOνA and T2K data combined, there are regions near $\delta' = 0$ or 180° where NSI solutions are allowed at less than 1σ; see the left panels of Fig. 3. So, although theoretically the degeneracies with NSI solutions should be resolved, the experimental uncertainties are large enough that large NSI regions are not excluded. Using the wide-band beam at DUNE, which effectively measures probabilities at a variety of energies, puts severe restrictions on NSI: $|\delta'| \lesssim 50°$ and $\epsilon \lesssim 0.1$ at 3σ for $\epsilon_{e\mu}$; see the top-right panel of Fig. 3. However, some small degenerate regions in $\delta' - \epsilon_{e\tau}$ space are allowed at less than 2σ due to the mass hierarchy degeneracy; see the bottom-right panel of Fig. 3. This can be understood from the oscillation probabilities shown in Fig. 4. The dashed curves almost

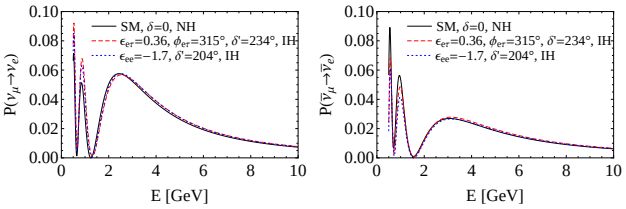

FIG. 4. $\nu_\mu \to \nu_e$ and $\overline{\nu}_\mu \to \overline{\nu}_e$ oscillation probabilities at DUNE. The mixing angles and mass-squared differences are the best-fit values in Ref. [12].

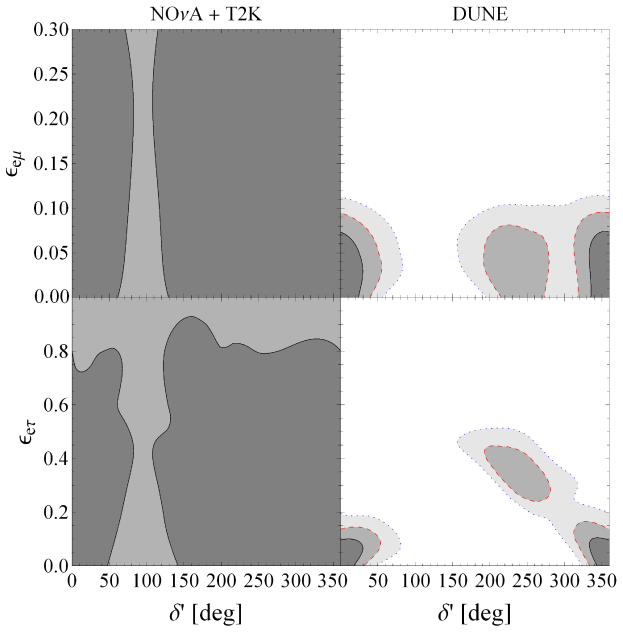

FIG. 5. Same as Fig. 3, except both $\epsilon_{e\mu}$ and $\epsilon_{e\tau}$ are nonzero.

overlap the SM curves in both the neutrino and antineutrino channels. This could lead to a wrong determination of the mass hierarchy and CP phase. Also, in parts of the allowed parameter-space, θ_{23} lies in the second octant which could lead to a wrong determination of the octant. We see that DUNE alone cannot completely resolve these degeneracies for nonzero $\epsilon_{e\tau}$.

Two off-diagonal NSI. If both $\epsilon_{e\mu}$ and $\epsilon_{e\tau}$ are nonzero, then there are five free NSI parameters: δ', two magnitudes, and two phases. Therefore, two ϵ's and P and $\overline{P}$ measurements at two different L and E combinations (four equations and five unknowns) will have potential NSI degeneracies for any δ and δ' (just as with one ϵ and P and $\overline{P}$ measurements at just one L/E). The corresponding allowed regions of $\epsilon_{e\mu}$ and $\epsilon_{e\tau}$ from combining the NOνA and T2K experiments are shown in Fig. 5; any value of δ' is allowed at less than 2σ. Therefore P and $\overline{P}$ measurements at a *third* L/E are in principle required to resolve the degeneracies. Alternatively, a wide-band beam experiment can be used. Figure 5 shows expected allowed regions from DUNE. As expected, DUNE cannot resolve all the degeneracies.

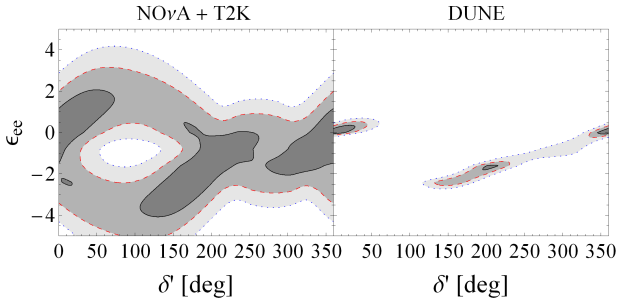

FIG. 6. Same as Fig. 3, except for ϵ_{ee}.

One diagonal NSI (ϵ_{ee}). In this case, the oscillation probability to second order is simply the first line of Eq. (4). Since $\phi_{ee} = 0$, there is a simple two-fold degeneracy between the SM and NSI, i.e., for measurement of P and $\overline{P}$ at one L/E, each value of δ is degenerate with a point (δ', ϵ_{ee}) in NSI space (although in some cases, due to the nonlinear nature of the equations, there are multiple, but finite number of degenerate solutions). In principle, a narrow-band beam experiment should be able to pinpoint both the SM value of δ and the degenerate NSI values of δ' and ϵ_{ee}. In practice, for NOνA and T2K, the uncertainties are too large and no value of δ' is strongly preferred; see Fig. 6. DUNE will put stronger constraints on NSI and δ'. The islands in the right panel of Fig. 6 can be understood from the dotted curves in Fig. 4. DUNE alone cannot resolve the mass hierarchy degeneracy, and it could also lead to a wrong determination of CP violation if ϵ_{ee} is $\mathcal{O}(1)$. Note that ϵ_{ee} does not affect the octant degeneracy.

In summary, we studied parameter degeneracies that occur in long-baseline neutrino appearance experiments due to matter NSI. We derived the oscillation probabilities for the appearance channels to second order in ϵ. We found that there is a continuous four-fold degeneracy for an off-diagonal NSI in narrow-band beam experiments like NOνA and T2K. A combination of their data would in principle break the degeneracy, but in practice, large regions of NSI parameter space remain allowed due to large experimental uncertainties. We also discussed degeneracies that occur for diagonal NSI, and for more than one off-diagonal NSI at a time. While the DUNE experiment can resolve most of the degeneracies, for nonzero $\epsilon_{e\tau}$ or ϵ_{ee}, there are some parameter regions in which DUNE could lead to a wrong determination of the mass hierarchy and of CP violation. Additionally, for nonzero $\epsilon_{e\tau}$ an incorrect conclusion about the octant of θ_{23} may be drawn. Nonzero ϵ_{ee} does not impact a resolution of the octant degeneracy. We conclude that DUNE alone cannot resolve all the degeneracies arising from NSI. (We did not consider the possibility of diagonal and off-diagonal NSI parameters being nonzero simultaneously, which leads to degeneracies between NSI parameters [9]. Clearly, this will further hinder the interpretation of DUNE data.) In this work we focused on how NSI may mimic the SM with CP conservation. In future work we consider degenera-

cies as a function of the CP phase [19].

Acknowledgments. KW thanks the University of Hawaii at Manoa for its hospitality in the initial stages of this work. This research was supported by the U.S. DOE under Grant No. DE-SC0010504.

[1] K. A. Olive *et al.* [Particle Data Group Collaboration], Chin. Phys. C **38**, 090001 (2014).
[2] T. Ohlsson, Rept. Prog. Phys. **76**, 044201 (2013) [arXiv:1209.2710 [hep-ph]].
[3] C. Biggio, M. Blennow and E. Fernandez-Martinez, JHEP **0908**, 090 (2009) [arXiv:0907.0097 [hep-ph]].
[4] L. Wolfenstein, Phys. Rev. D **17**, 2369 (1978).
[5] K. Abe *et al.* [T2K Collaboration], Nucl. Instrum. Meth. A **659**, 106 (2011) [arXiv:1106.1238 [physics.ins-det]].
[6] D. S. Ayres *et al.* [NOvA Collaboration], hep-ex/0503053.
[7] C. Adams *et al.* [LBNE Collaboration], arXiv:1307.7335 [hep-ex]; R. Acciarri *et al.* [DUNE Collaboration], arXiv:1512.06148 [physics.ins-det].
[8] J. A. B. Coelho, T. Kafka, W. A. Mann, J. Schneps and O. Altinok, Phys. Rev. D **86**, 113015 (2012) [arXiv:1209.3757 [hep-ph]]; R. Adhikari, S. Chakraborty, A. Dasgupta and S. Roy, Phys. Rev. D **86**, 073010 (2012) [arXiv:1201.3047 [hep-ph]]; A. Friedland and I. M. Shoemaker, arXiv:1207.6642 [hep-ph]; M. Masud, A. Chatterjee and P. Mehta, arXiv:1510.08261 [hep-ph]; A. de Gouvea and K. J. Kelly, arXiv:1511.05562 [hep-ph].
[9] P. Coloma, arXiv:1511.06357 [hep-ph].
[10] V. Barger, D. Marfatia and K. Whisnant, Phys. Rev. D **65**, 073023 (2002) [hep-ph/0112119].
[11] J. Kopp, M. Lindner, T. Ota and J. Sato, Phys. Rev. D **77**, 013007 (2008) [arXiv:0708.0152 [hep-ph]].
[12] M. C. Gonzalez-Garcia and M. Maltoni, JHEP **1309**, 152 (2013) [arXiv:1307.3092].
[13] P. Huber, M. Lindner and W. Winter, Comput. Phys. Commun. **167**, 195 (2005) [hep-ph/0407333]; P. Huber, J. Kopp, M. Lindner, M. Rolinec and W. Winter, Comput. Phys. Commun. **177**, 432 (2007) [hep-ph/0701187].
[14] J. Kopp, Int. J. Mod. Phys. C **19**, 523 (2008) [physics/0610206]; J. Kopp, T. Ota and W. Winter, Phys. Rev. D **78**, 053007 (2008) [arXiv:0804.2261 [hep-ph]].
[15] P. Huber, M. Lindner, T. Schwetz and W. Winter, JHEP **0911**, 044 (2009) [arXiv:0907.1896 [hep-ph]].
[16] J. M. Berryman, A. de Gouvea, K. J. Kelly and A. Kobach, Phys. Rev. D **92**, no. 7, 073012 (2015) [arXiv:1507.03986 [hep-ph]].
[17] A. M. Dziewonski and D. L. Anderson, Phys. Earth Planet. Interiors **25**, 297 (1981).
[18] R. J. Geller and T. Hara, Nucl. Instrum. Meth. A **503**, 187 (2003) [hep-ph/0111342].
[19] J. Liao, D. Marfatia and K. Whisnant, in progress.